Transparency of an overdense plasma layer

Baifei Shen and Zhizhan Xu
Shanghai Institute of Optics and Fine Mechanics, P. O. Box 800-211, Shanghai 201800, China
(Received 28 April 2001; published 23 October 2001)

The transition from opacity to transparency of overdense plasma layers for the propagation of high-intensity laser pulses of circular polarization is investigated theoretically and by simulation. We discuss in detail the regions where stationary solutions exist and therefore the plasma layer is opaque. We find that the opacity depends not only on the electron density and the laser intensity but also on the thickness of the plasma layer. We also discuss the overlap region where both transparency and opacity are possible and how it depends on the history. Ion acceleration is studied in both the opacity region and the transparency region.

DOI: 10.1103/PhysRevE.64.056406 PACS number(s): 52.27.Ny, 52.38.Kd, 52.65.Rr

I. INTRODUCTION

The propagation of an intense laser pulse in a plasma layer is of interest both for understanding laser plasma interaction [1] and for applications such as electron accelerators [2–5], x-ray lasers [6], and the fast ignitor concept for inertial confinement [7]. The interaction of intense laser pulses with different plasma densities has been widely investigated. For a density much larger than the critical density $n_c = 1.1\times 10^{21}\ \lambda^2\ \mu\mathrm{m}^{-2}\ \mathrm{cm}^{-3}$, most of the laser pulse usually reflects from the plasma surface when the laser pulse is normally incident. High-order harmonics [8,9], energetic electrons [10], and ions have been observed [11,12]. Boring and static magnetic fields have also been investigated [13]. In the case of ultrathin foil, a large part of the laser pulse can penetrate through the foil, but it is still by means of an evanescent wave. For an underdense plasma, a laser pulse propagates in the plasma while instabilities such as backward Raman scattering, forward Raman scattering, and modulational instability can occur. Self-focusing occurs when an intense laser pulse of power higher than $17(n_c/n_e)$ GW propagates in a plasma. Energetic electrons are generated by direct laser acceleration and the wakefield [3,4]. A strong static magnetic field is produced by the accelerated electrons [5]. For a plasma with density slightly larger than the critical density, induced transparency is possible because the plasma frequency is reduced by the relativistic factor γ of an electron in the laser field [14–19].

The transition between opacity and transparency has been investigated analytically [14,15,19] and by particle-in-cell (PIC) simulations [17]. For fixed ions, Kaw and Dawson [14] estimated the critical strength for the transition as $a_{lin} = 4n/(\pi n_c)$ for linear polarization and $a^2_{circ} = (n/n_c)^2 - 1$ for circular polarization, where $a = eA/mc^2$ is the laser amplitude in the plasma. However, the transit point from transparency to opacity is still not clearly defined. We note that in practice the laser pulse illuminates a plasma layer of finite thickness and therefore the laser field in the plasma differs from the laser field in vacuum. Due to the light pressure, the electron density is no longer homogeneous.

In this paper we discuss this transit point analytically and by simulations. At some points, fluid equations cannot give a stationary solution, and then the kinetic aspects of the interaction should be considered. At the same time the plasma layer begins to change from opacity to transparency. Therefore, we define the point at which a stationary solution no longer exists as the point at which the plasma layer changes from opacity to transparency or absolute transparency. We find that this transition depends on the plasma density, laser intensity, and also the thickness of the plasma layer. The dependence on the plasma thickness, to our knowledge, has not been studied before. We also study the overlap region where both transparency and opacity are possible as proposed by Goloviznin and Schep [19]. In this region, a stationary solution for opacity still exist, and it depends on the history whether the plasma layer is transparent or opaque. This is confirmed by one dimensional PIC simulations based on the code LPIC++ [20].

II. FORMULATION

We consider only one dimensional geometry as illustrated in Fig. 1. One planar laser pulse illuminates an overdense plasma laser normally. In order to obtain an analytical solution easily, all of the analyses are based on circularly polarized laser pulses. In the interaction of ultrashort laser pulses of high contrast with a plasma, ions react on a longer time scale than electrons and are therefore treated as a motionless background. Because the electron thermal velocity is much smaller than the quiver velocity, the plasma can be treated as cold. Analytical studies of strong electromagnetic waves

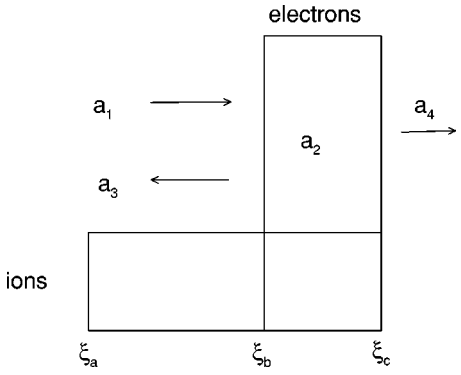

FIG. 1. Schematic drawing of electron and ion density of the plasma layer with ξ_a, ξ_b, ξ_c marking left and right layer boundaries and a_1, a_2, a_3, a_4 defining wave amplitudes.

propagating in a cold overdense plasma are generally based on Maxwell's equations and the relativistic equation of motion for electrons [14,15,21–24]

We and others have successfully used this method for laser interactions with solids and foils of solid density with the help of boundary conditions [19,24]. In order to discuss the method easily, we repeat some of the main results in this section. We are looking for stationary solutions for which the longitudinal electron velocity vanishes. The incident circularly polarized laser pulse propagating in the z direction has the form $a_1 = a_1 e^{i(\omega_L t - k_L z)}$. Letting the wave field in the plasma have the form $a_2 = a_2(\xi) e^{i\omega_L t + i\theta(\xi)}$ with real amplitude $a_2(\xi)$ and real phase $\theta(\xi)$, we obtain two ''constants of motion'' with respect to the variation in ξ [21,24]:

$$M = -(\partial\theta/\partial\xi)(\gamma^2 - 1), \tag{1}$$

$$W = [(\partial\gamma/\partial\xi)^2 + M^2]/2(\gamma^2 - 1) + \gamma^2/2 - N_i\gamma, \tag{2}$$

where $a = eA/mc^2$, $\xi = k_L z$, $\gamma = (1 + a^2)^{1/2}$, and $N_i = n_i/n_c$; n_i and n_c are the ion density and critical density, respectively. The constant M describes the net flow of the laser pulse. For the case of complete reflection $M = 0$, while for the case of complete transparency $M = \gamma^2 - 1$. In order to obtain the solution of the equations, we have to consider boundary conditions. From the continuity conditions of transverse electric and magnetic fields at the left and right surfaces of the electron layer, we derive

$$2(a_1^2 + a_3^2) = (\partial a_b/\partial\xi)^2 + M^2/a_b^2 + a_b^2, \tag{3}$$

$$M = a_1^2 - a_3^2, \tag{4}$$

$$W = |M| + 1/2 - N_i(|M| + 1)^{1/2}, \tag{5}$$

where a_3 is the amplitude of the reflected wave and a_b is the amplitude at the inner side of the left surface. Because electron motion in the longitudinal direction can be neglected, we obtain the normalized static electric field

$$E_z = -\partial\gamma/\partial\xi = \pm[(2W + 2N_i\gamma - \gamma^2)(\gamma^2 - 1) - M^2]^{1/2}. \tag{6}$$

Therefore, the thickness of the electron layer is given by means of the integral $\xi_{bc} = \int(-1/E_z)d\gamma$. The thickness of the ion layer on the left side of the foil is given by $N_i\xi_{ab} = -E_z(\xi_b)$ with the help of the continuity condition of the longitudinal electric field. We also find that the electron density

$$N_e = \gamma(3N_i\gamma - 2\gamma^2 + 1 + 2W). \tag{7}$$

III. STATIONARY SOLUTIONS

The stationary solution given in Sec. II can be obtained only when some conditions are satisfied. Here we give the conditions. We find that the conditions are the same as the conditions for transparency. From Eqs. (2) and (3) we obtain at the left surface of the electron layer

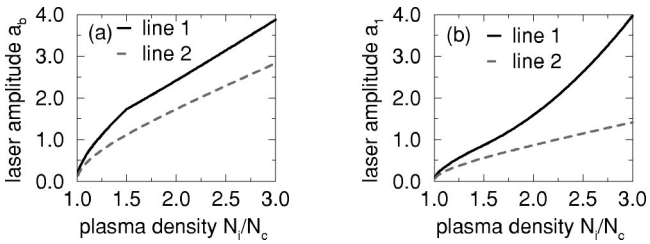

FIG. 2. The line 1 in (a) and (b) divides the region of absolute transparency (above line 1) from others for a half infinite plasma layer. The line 2 in (a) and (b) divides the region of absolute opacity (below line 2) from others. The laser amplitude is normalized as $a = eA/mc^2$.

$$y = 4a_1^2 - 2M + M^2 - \gamma_b^2 + 1 - 2W\gamma_b^2 - 2N_i\gamma_b^3 + \gamma_b^4 = 0, \tag{8}$$

$$2(2a_1^2 - M) \leqslant M^2/a_b^2 + a_b^2, \tag{9}$$

$$(2W + 2N_i - \gamma_b - \gamma_b^2)(\gamma_b^2 - 1) \leqslant M^2; \tag{10}$$

y has an extreme value when $\partial y/\partial\gamma_b = 0$, i.e.,

$$2\gamma_b^2 - 3N_i\gamma_b - (2W + 1) = 0. \tag{11}$$

In order that the above equation (8) has a solution, from Eq. (11) we find that

$$\gamma_b \leqslant \gamma_{bc} = [3N_i + (9N_i^2 + 16W + 8)^{1/2}]/4. \tag{12}$$

In the case of complete reflection, which means that the plasma layer is half infinite and the electron density is sufficiently large, $M = 0$. From Eqs. (8)–(12) we find that at the left surface of the electron layer

$$y_0 = 4a_1^2 + 1 - (2 - 2N_i)\gamma_b^2 - 2N_i\gamma_b^3 + \gamma_b^4 = 0, \tag{13}$$

$$\gamma_b \leqslant \gamma_{bc} = 2N_i - 1, \tag{14}$$

$$\gamma_b \leqslant \gamma_{bc} = [3N_i + (9N_i^2 - 16N_i + 16)^{1/2}]/4. \tag{15}$$

The two lines [Eqs. (14) and (15)] cross at $N_i = 1.5$. So we have

$$\gamma_b \leqslant \gamma_{bc} = 2N_i - 1, \quad 1 \leqslant N_i \leqslant 1.5, \tag{16}$$

$$\gamma_b \leqslant \gamma_{bc} = [3N_i + (9N_i^2 - 16N_i + 16)^{1/2}]/4, \quad N_i \geqslant 1.5. \tag{17}$$

With the help of Eq. (13), we plot the line 1 for the amplitude in vacuum a_1 and the amplitude inside the electron layer a_b $(= \sqrt{\gamma_b^2 - 1})$ in Figs. 2(a) and 2(b). It is for half infinite plasma layers.

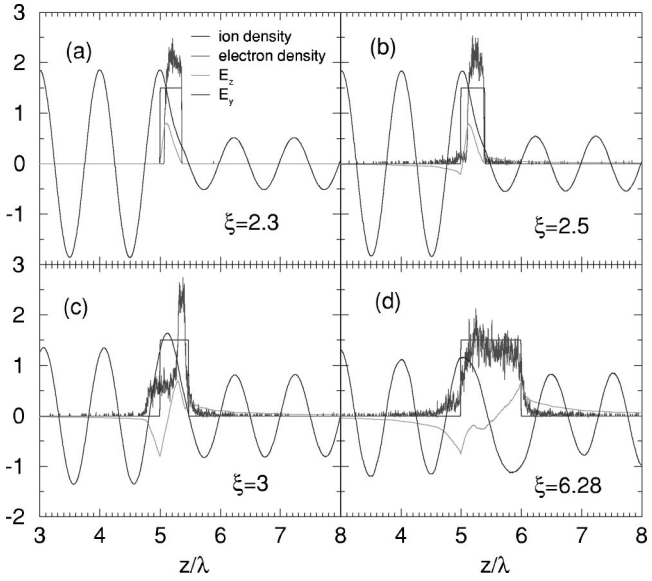

FIG. 3. Snapshots after 120 laser cycles for interactions between a laser pulse, which rises from $a_1=0$ to $a_1=1$ in 15 laser cycles and then remains constant, and plasma layers of normalized density $N_i=1.5$ and thickness $\xi_{ac}=$ (a) 2.3, (b) 2.5, (c) 3, and (d) 6.28. The plasma layer is at $\xi_a/2\pi=5$. The electric field is normalized as $E=eE/m\omega c$.

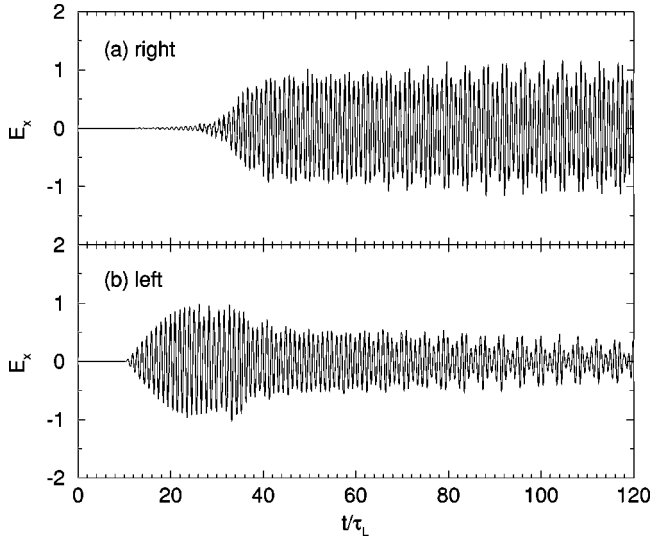

FIG. 4. The transmitted (a) and reflected (b) waves at the right side ($\xi/2\pi=11$) and the left side ($\xi=0$) of the simulation box. The laser pulse and the plasma layer are the same as in Fig. 3(d). The time is normalized to the laser cycle.

For $N_i \leqslant 1.5$ and $a_1=\sqrt{N_i(N_i-1)}$ ($\gamma_b=2N_i-1$), the ponderomotive force at the surface of the electron layer is zero. Therefore, the electrons can reach the surface of the ions, where the laser amplitude inside the plasma is twice as large as the laser amplitude in vacuum.

Now we discuss the results in different domains.

A. $N_i=1.5$

From Eqs. (16) and (17), we find the critical relativistic factor $\gamma_{bc}=2$ for a plasma density of $N_i=1.5$ in the case of $M=0$. From Eq. (13), we obtain the corresponding critical amplitude in vacuum $a_{1c}=\sqrt{3}/2$. Therefore, $a_1=\sqrt{3}/2$ means that we have $M=0$ and a stable half infinite plasma layer. From Eq. (6) we also have $\xi_{ab}=(\partial\gamma/\partial\xi)|_{\xi=\xi_b}/N_i=0$, which means that the surface of the electron layer is the same as that of the ion layer. From Eq. (7), we have $N_b=0$. It should be mentioned that this situation was studied by Goloviznin and Schep [19].

When $a_1>\sqrt{3}/2$, there is no stable solution for $M=0$. This means that there are stable solutions only for finite plasma layers. From Eqs. (5), (6), (8), and (11), we can obtain the largest thickness of the plasma layer that supports a stable solution. For example, when $a_1=1$, in Eqs. (5), (8), and (11) there are three variables M, W, and γ_b. So it is easy to obtain the smallest constant $M=0.24$. Here Eq. (11) is important. Only with the help of Eq. (11) do we have a definite solution for the largest thickness of foil. Then from Eq. (6) we obtain the corresponding largest thickness as $\xi_{ac}=2.4$. When $\xi_{ac}>2.4$, there is no stable solution. In order to confirm the analytical solution, we performed PIC simulations for plasma layers of density $N_i=1.5$. The laser pulse rises from $a_1=0$ to $a_1=1$ in 15 laser periods and then stays constant. The thicknesses of the plasma layer are $\xi_{ac}=2.3,\ 2.5,\ 3$, and 6.28. Snapshots after 120 laser cycles are plotted in Fig. 3. For the plasma layer of thickness $\xi_{ac}=2.3$, we have a stationary solution as predicted analytically. Part of the laser pulse propagates through the plasma layer by means of an evanescent wave. For the plasma layer of thickness $\xi_{ac}=2.5$, where we expect no stationary solution, the kinetic aspect of the interaction has become important, and the plasma layer has begun to change from opacity to transparency. So no stationary solution means that the kinetic aspect of the interaction becomes important. It is interesting that this is related to the problem of transparency. For the plasma layer of thickness $\xi_{ac}=6.28$, almost all of the laser pulse propagates through the plasma layer. Therefore, it is not a sudden change from opacity to transparency. When the foil becomes thicker or when the laser amplitude becomes larger for a given thickness, the foil becomes more and more transparent. This differs from the case of nonrelativistic laser pulses. Dynamically, it takes time for the plasma layer to become transparent to the laser pulses as reported by Guerin *et al.* [16]. We plot the wave field at both left and right surfaces of the simulation box as a function of time in Fig. 4. The parameters are the same as in Fig. 3(d). It shows that at the beginning, the laser pulse is mainly reflected and then mainly transmitted. It is interesting that the laser pulse has a minimum transmission for a plasma layer of thickness $\xi_{ac}=2.4$. When $\xi_{ac}<2.4$, a thinner plasma layer means a shorter decay distance of the evanescent wave. When $\xi_{ac}>2.4$, a thicker layer means approaching more closely to a complete transparency. It should be mentioned that the laser field at the left side of the foil, in Fig. 3, is a sum of the incident and reflected waves. We plot here only E_y, while E_x, B_y, and B_x do not appear in the figure.

When $a_1<\sqrt{3}/2$, there is always a stable solution for any thickness.

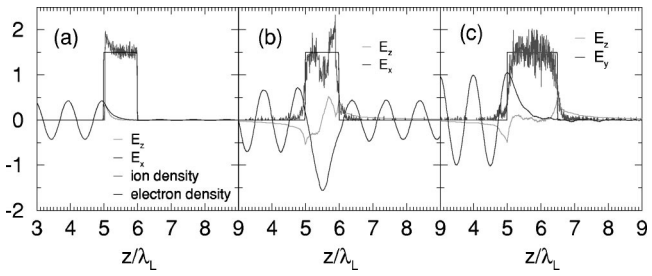

FIG. 5. Snapshots after 120 laser cycles for interactions between laser pulses and plasma layers of density $N_i=1.5$. (a) The laser pulse rises from $a_1=0$ to $a_1=0.5$ in five laser cycles and then remains constant. The plasma layer is of thickness λ_L or $\xi_{ac}=6.28$. (b) The laser pulse rises from $a_1=0$ to $a_1=1$ before it decrease to $a_1=0.5$ and then remains constant. The plasma thickness is the same as in (a). (c) The laser pulse is the same as in (b) and the plasma layer is of thickness $1.5\lambda_L$. The electric field is normalized as $E=eE/m\omega c$.

B. $N_i>1.5$

From Eq. (17) we know that only when $\gamma_b<\gamma_{bc}=[3N_i+(9N_i^2-16N_i+16)^{1/2}]/4$ is there a stationary solution for a half infinite plasma layer, i.e., $M=0$. With the help of Eq. (13), we find that $a_1<a_{1c}=[2N_i(\gamma_b^3-\gamma_b^2)-(\gamma_b^2-1)^2]^{1/2}/2$. When $a_1<a_{1c}$, there is a solution for a half infinite plasma layer and there are solutions for any finite thickness. When $a_1>a_{1c}$ there are stable solutions only for finite plasma layers. Supposing that a_1 and N_i are given, the smallest M is again determined by Eqs. (5), (8), and (11). The smallest M corresponds to the largest thickness of the plasma layer. For example, for $N_i=2$, $\gamma_{bc}=2.618$, $a_{1c}=1.588$, when $a_1=2>a_{1c}$, the smallest $M=1.5584$ and the largest thickness is $\xi_{ac}=1.99$. Therefore, when $\xi_{ac}>1.99$, the plasma layer begins to become transparent.

C. $N_i<1.5$

From Eq. (16), we find that there is a stationary solution for a plasma layer of half infinite thickness only when $\gamma_b\leqslant\gamma_{bc}=2N_i-1$. Therefore, $a_1<a_{1c}=\sqrt{N_i(N_i-1)}$. For example, for $N_i=1.2$, when $\gamma_b<1.4$, i.e., $a_1<0.49$, there is a stationary solution for a half infinite plasma layer. When $\gamma_b>2N_i-1$, there is a stationary solution only for a plasma layer of finite thickness, and there are two different regions as seen in Fig. 2. When $2N_i-1<\gamma_b<[3N_i+(9N_i^2+16W+8)^{1/2}]/4$, the largest thickness is determined by Eqs. (5), (9), and (10) and $(\partial\gamma/\partial\xi)_b=0$ for Eq. (6). At the point b, for a stationary solution $(\partial\gamma/\partial\xi)_b<0$ so that the ponderomotive force balances the static electric force. If $(\partial\gamma/\partial\xi)_b>0$, both ponderomotive force and static electric force have the same direction. Therefore, a stationary solution cannot exist. For example, for $N_i=1.2$ and $a_1=0.51$, we have $M=0.011$, $\gamma_b=1.421$, and the largest thickness of the plasma layer $\xi_{ac}=5.51$. This is inside the region $1.4<\gamma_b<1.68$. When $\gamma_b>[3N_i+(9N_i^2+16W+8)^{1/2}]/4$, the largest thickness is determined by Eqs. (5), (8), and (11).

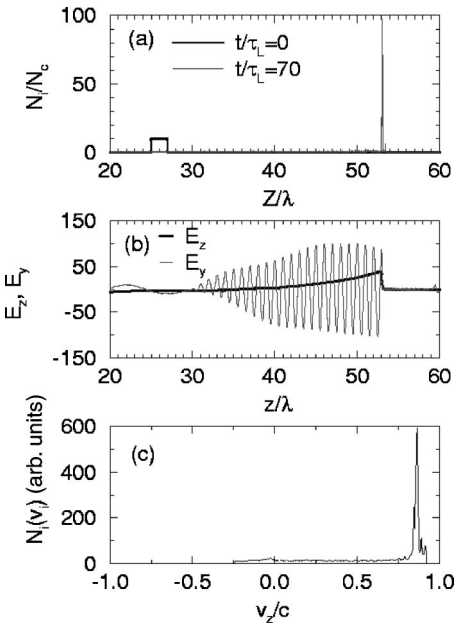

FIG. 6. The ion density distribution (a), normalized laser and static electric field (b), and ion velocity distribution (c) after 70 laser cycles. The plasma layer of density $N_i=10$ and thickness $2\lambda_L$ is initially at $\xi/2\pi=25$. The laser pulse is $a_1=100[\sin(\phi_1)\hat{x}+\cos(\phi_1)\hat{y}]\sin(\phi_1/80)$, $0<\phi_1=\omega_L t-k_L z\leqslant 80\pi$.

IV. TRANSPARENCY

When the above conditions are not satisfied, self-induced transparency is found in the PIC simulations [16–18]. We call it absolute transparency in order to distinguish it from the regions described below. In the case of transparency, instabilities always occur [25–27]. When all or part of the electrons are heated, the growth rate of the instabilities is

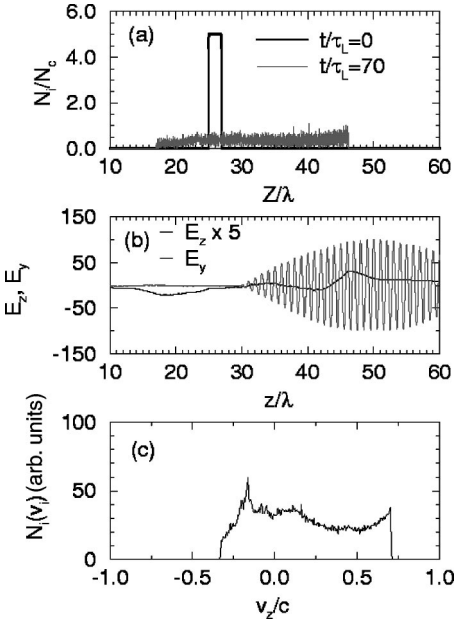

FIG. 7. Same as in Fig. 6 but for a plasma layer of density $N_i=5$.

reduced significantly [25,26]. Guerin *et al.* believe that laser pulses can propagate due to the reduced growth rate [16]. However, self-induced transparency could also happen even when the conditions for a stationary solution are satisfied. In Sec. III, our starting point is opacity. We try to find when the stationary solution for opacity no longer exists. In this section our starting point is transparency. We try to find when the conditions for transparency are no longer satisfied. In order to obtain the conditions for this transparency, we neglect the instabilities. We know that in the case of transparency almost all of the laser pulse transmits through the plasma layer. So the electron density experiences little change because of small light pressure. Therefore, the dispersion relation is

$$k_0^2=\omega_L^2-\omega_p^2/\gamma, \tag{18}$$

where γ is the Lorentz factor of the electrons in the plasma layer, which can be larger than the Lorentz factor in vacuum. In the plasma layer we should have $\gamma>N_i$ for the case of transparency. From Eq. (9) we find that

$$a_1^2>(N_i^2-1)/4. \tag{19}$$

So we obtain the second condition for transparency. This is a condition for plasma layers of any thickness. The amplitude a_1 in vacuum and a_b obtained here are also plotted as line 2 in Fig. 2. One observes that the conditions obtained here by Eq. (19) differ from the conditions obtained above by Eqs. (16) and (17) and these two regions overlap. This means that in some region both opacity and transparency are possible.

In order to confirm the overlap region of transparency and opacity, we performed simulations for a plasma of density $N_i=1.5$. The thickness of the plasma layer is λ_L or $\xi_{ac}=6.28$ for Figs. 5(a) and 5(b) and $1.5\lambda_L$ for Fig. 5(c). The laser amplitude is $a_1=0.5$. For Fig. 5(a), the amplitude of the laser pulse rises from 0 to 0.5 in five laser cycles and then stays constant, i.e.,

$$a_1=\begin{cases}[\sin(\phi_1)\hat{x}+\cos(\phi_1)\hat{y}]\sin(\phi_1/60), & 0<\phi_1=\omega_L t-k_L z\leqslant 10\pi,\\ 0.5, \quad \phi_1>10\pi.\end{cases} \tag{20}$$

For Figs. 5(b) and 5(c), the amplitude of the laser pulse first rises to $a_1=1$, then decreases to $a_1=0.5$, and then stays constant, i.e.,

$$a_1=\begin{cases}[\sin(\phi_1)\hat{x}+\cos(\phi_1)\hat{y}]\sin(\phi_1/60), & 0<\phi_1=\omega_L t-k_L z\leqslant 50\pi,\\ 0.5, \quad \phi_1>50\pi.\end{cases} \tag{21}$$

We give the result after 120 laser cycles. In Fig. 5(a), the simulation gave a stationary result like the analytical result for opacity. The laser pulse is almost completely reflected. But, in Fig. 5(b) a laser pulse of the same amplitude can propagate through a plasma layer of the same thickness. Notice that $a_1=0.5$ is lower than the value $a_1=0.56$ given by Eq. (19) for $N_i=1.5$. Because the electron density has been reduced due to electrons moving out of the plasma layer, a laser pulse of this low amplitude can propagate in a plasma layer of initial electron density $N_i=1.5$. In Fig. 5(c), the plasma layer is thicker than in Fig. 5(b). The influence of the outgoing electrons, therefore, becomes small. One observes that the plasma layer returns to opacity. With PIC simulations, we confirm that it is dependent on the history whether a plasma is transparent or opaque in the overlap region.

In conclusion, at the front of a laser pulse, when the laser amplitude is larger than line 1 in Fig. 2(a), the plasma begins to become transparent; at the back of the pulse, when the laser amplitude is smaller than line 2 in Fig. 2(a), the plasma begins to become opaque.

V. ION ACCELERATION

Driven by the large longitudinal electric static field, ions move, although on a longer time scale. For a thin foil, electrons move first due to the large light pressure; then ions follow pulled by the electric static field, leaving a long plasma tail of low density, because the electric static field has a maximum always at the surface of the electron layer. We performed a simulation for a plasma layer of density $N_i=10$ and thickness $2\lambda_L$ ($\xi=4\pi$). The plasma layer is initially at $\xi_a/2\pi=25\lambda_L$. The laser pulse, $a_1=100[\sin(\phi_1)\hat{x}+\cos(\phi_1)\hat{y}]\sin(\phi_1/80)$, $0<\phi_1=\omega_L t-k_L z\leqslant 80\pi$, has a peak amplitude $a=100$ after 20 laser cycles. Ion density, laser field E_x, and longitudinal electric field are given in Figs. 6(a) and 6(b). It is shown that the ion layer is accelerated as a single entity by the longitudinal electric field or indirectly by the light pressure. We stress that a laser pulse of amplitude $a_1=100$ can reflect completely from a plasma layer of initial density $N_i=10$ because of the high electron and ion density compressed by the light pressure. A simulation was also done for the same conditions as in Fig. 6 but lower density $N_i=5$. Now the laser pulse can propagate through the plasma layer and therefore the light pressure is no longer important. Electrons are still accelerated mainly in the forward direction, but also in the backward direction due to instabilities, wakefield, and direct laser acceleration. Then some ions, mainly near the surface of the ion layer, are ac-

celerated by the strong static electric field. From Fig. 7, one observers that the ion density distribution and ion velocity distribution are much different from those in Fig. 6. It is of interest that there is an apparent cutoff in the ion velocity distribution. So the ion acceleration is very different for the cases of transparency and opacity.

VI. CONCLUSIONS

In conclusion, a laser pulse of circular polarization can propagate in plasmas when $\omega_L^2 > \omega_p^2/\gamma$, where γ is the Lorentz factor of the electrons in the plasma. However, the problem is complex for finite or half infinite plasma layers, because the electron density can be modified by the ponderomotive force and the Lorentz factor γ in plasmas differs from γ in vacuum. Stationary solutions and the regions where the stationary solutions exist have been obtained for half infinite plasma layers and also for finite ones. In these regions, the plasma layers can be opaque to the laser pulses. Beyond these regions, the plasma layers become transparent, defined as absolute transparency. By seeking the region of transparency by another method, it is found that even part of the region where a stationary solution exists may be transparent. Therefore, there is an overlap between the regions of transparency and opacity, where both transparency and opacity are possible. Dynamically, it takes time, sometimes a long time, for a plasma layer to become transparent even in the region of absolute transparency. Ion motion must be considered for longer laser pulses. In the region of opacity, both electrons and ions in a thin plasma layer can be accelerated by the light pressure. Therefore, the plasma layer moves as a whole. In the region of transparency, electrons are accelerated by many mechanisms and move out of the plasma layer, so ions are accelerated due to the strong static electric field.

ACKNOWLEDGMENTS

This work was supported by the Shanghai Venus Program. The code LPIC++ was run on SW-I at the Shanghai Computer Center.

[1] W. Kruer, *The Physics of Laser-Plasma Interactions* (Addison-Wesley, New York, 1988).
[2] G. Malka, J. Fuchs, F. Amiranoff, S. D. Baton, R. Gailard, J. L. Miquel, H. Pepin, C. Rousseaux, G. Bonnaud, M. Busquet, and L. Lours, Phys. Rev. Lett. **79**, 2053 (1997).
[3] A. Pukhov, Z. M. Sheng, and J. Meyer-ter-Vehn, Phys. Plasmas **6**, 2847 (1999).
[4] C. Gahn, G. D. Tsakiris, A. Pukhov, J. Meyer-ter-Vehn, G. Pretzler, P. Thirolf, D. Habs, and K. J. Witte, Phys. Rev. Lett. **83**, 4772 (1999).
[5] A. Pukhov and J. Meyer-ter-Vehn, Phys. Rev. Lett. **76**, 3975 (1996).
[6] R. Elton, *X-Ray Lasers* (Academic Press, London, 1990).
[7] M. Tabak, J. Hammer, M. E. Glinsky, W. L. Kruer, S. C. Wilks, J. Woodworth, E. M. Campbell, M. D. Perry, and R. J. Mason, Phys. Plasmas **1**, 1626 (1994).
[8] P. A. Norreys, M. Zepf, S. Moustaizis, A. P. Fews, J. Zhang, P. Lee, M. Bakarezos, C. Danson, A. Dyson, P. Gibbon, P. Loukakos, D. Neely, F. Walsh, J. Wark, and A. Dangor, Phys. Rev. Lett. **76**, 1832 (1996).
[9] R. Lichters, J. Meyer-ter-Vehn, and A. Pukhov, Phys. Plasmas **3**, 3425 (1996).
[10] A. Pukhov and J. Meyer-ter-Vehn, Phys. Rev. Lett. **79**, 2686 (1997).
[11] K. Krushelnick, E. L. Clark, M. Zepf, J. R. Davies, F. N. Beg, A. Machacek, M. I. Santala, M. Tatarakis, I. Watts, P. A. Norreys, and A. E. Danger, Phys. Plasmas **7**, 2055 (2000).
[12] T. E. Cowan, A. W. Hunt, T. W. Phillips, S. C. Wilks, M. D. Perry, C. Brown, W. Fountain, S. Hatchett, J. Johnson, M. H. Key, T. Parnell, D. M. Pennington, R. A. Shavely, and Y. Takahashi, Phys. Rev. Lett. **84**, 903 (2000).
[13] J. Fuchs, J. C. Adam, F. Amiranoff, S. D. Baton, N. Blanchot, P. Gallant, L. Gremillet, A. Heron, J. C. Kieffer, G. Laval, G. Malka, J. L. Miquel, P. Mora, H. Pepin, and C. Rousseaux, Phys. Plasmas **6**, 2563 (1999).
[14] P. Kaw and J. Dawson, Phys. Fluids **13**, 472 (1970).
[15] C. Max and F. Perkins, Phys. Rev. Lett. **27**, 1342 (1971).
[16] S. Guerin, P. Mora, J. C. Adam, A. Heron, and G. Laval, Phys. Plasmas **3**, 2693 (1996).
[17] E. Lefebvre and G. Bonnaud, Phys. Rev. Lett. **74**, 2002 (1995).
[18] H. Sakagami and K. Mima, Phys. Rev. E **54**, 1870 (1996).
[19] V. V. Goloviznin and T. J. Schep, JETP Lett. **70**, 450 (1999); Phys. Plasmas **7**, 1564 (2000).
[20] R. Lichters, R. E. W. Pfund, and J. Meyer-ter-Vehn, computer code LPIC++ Report MPG225, MPI Quantenoptik, Garching, 1997.
[21] C. S. Lai, Phys. Rev. Lett. **36**, 966 (1976).
[22] Wei Yu, M. Y. Yu, Z. M. Sheng, and J. Zhang, Phys. Rev. E **58**, 2456 (1998).
[23] R. N. Sudan, Phys. Rev. Lett. **70**, 3075 (1993).
[24] Baifei Shen and J. Meyer-ter-Vehn, Phys. Plasmas **8**, 1003 (2001).
[25] S. Guerin, G. Laval, P. Mora, J. C. Adam, and A. Heron, Phys. Plasmas **2**, 2807 (1995).
[26] Z.-M. Sheng, K. Mima, Y. Sentoku, and K. Nishihara, Phys. Rev. E **61**, 4362 (2000).
[27] A. S. Sakharov and V. I. Kirsanov, Phys. Rev. E **49**, 3274 (1994).